

Poly(propylene glycol)-Based Non-Isocyanate Polyurethane Ionenes: Thermal, Morphological and Conductive Properties

Jordan C. Pierce, George M. Timmermann, Creston Singer, David Salas-de la Cruz, and Kevin M. Miller*

The synthesis and characterization of a series of polyurethane ionenes using a non-isocyanate approach is disclosed. Imidazole-capped, urethane-containing prepolymers are prepared by first reacting carbonyl diimidazole (CDI) with several poly(propylene glycol) (PPG) diols with variable molecular weight, followed by subsequent reaction with 3-aminopropylimidazole (API). Polymerization with 1,4-dibromomethylbenzene followed by anion exchange resulted in the desired polyurethane ionenes bearing the [NTf₂] counteranion as a series of viscous liquids. NMR and FTIR spectroscopy are used to characterize the intermediates and final ionenes, including molecular weight determination by end-group analysis. A single glass transition temperature (T_{σ}) , as determined by differential scanning calorimetry (DSC), is observed for each ionene (-38 to -64 °C) with the T_g decreasing with increasing PPG molecular weight. Thermogravimetric analysis (TGA) indicated a two-step decomposition for each ionene, with the first being degradation of the PPG segment, followed by the urethane/ionic segment. Microphase separation is observed from x-ray scattering profiles with Bragg distances that increased with increasing PPG molecular weight. Ionic conductivity is found to be inversely dependent upon DSC T_{σ} at lower temperatures (RT and below); however, at higher temperatures, conductivity appears to be more dependent upon the ability of ionic aggregates caused by phase separation to interact.

1. Introduction

Since they were first disclosed in the 1930s, polyurethanes (PUs) remain as one of the most heavily used commercial polymers due to their broad range of thermal and mechanical properties.^[1] The

J. C. Pierce, G. M. Timmermann, K. M. Miller
Department of Chemistry
Murray State University
Murray, KY 42071, USA
E-mail: kmiller38@murraystate.edu
C. Singer, D. Salas-de la Cruz
Center for Computational and Integrative Biology
Rutgers University
Camden, New Jersey 08102, USA
D. Salas-de la Cruz
Department of Chemistry
Rutgers University
Camden, New Jersey 08102, USA

The ORCID identification number(s) for the author(s) of this article can be found under https://doi.org/10.1002/macp.202300290

DOI: 10.1002/macp.202300290

reaction between an alcohol and an isocyanate is often rapid and exothermic. As a result, applications of polyurethanes are also broad in scope and include adhesives, foams (rigid and flexible), coatings, and elastomers. Currently, the most common route used for making commercial polyurethanes involves a two-step "prepolymer" process. First, a polyol is reacted with an excess of low molecular weight diisocyanate, creating an isocyanateterminated prepolymer, followed by reaction in the second step with another polymer (chain extender or crosslinking agent), resulting in the final PU. The variability in isocyanate and polyols which are commercially available have led to the aforementioned array of properties.

The synthesis of polyurethanes via an isocyanate route comes with various hazards. First of all, the synthesis of the low molecular weight isocyanates from amines requires the use of phosgene, a highly toxic gas. Secondly, two of the most common commercial isocyanates, TDI (toluene diisocyanate) and MDI (methylene diphenylisocyanate) are not only toxic

but also carcinogenic.^[2,3] While the isocyanate-terminated prepolymers formed from the reaction of these low molecular weight isocyanate monomers with polyols reduces their toxicity profile, they still bear a very reactive functional group. Additionally, even at the end of their lifetime, PUs have been found to degrade into isocyanates and hydrogen cyanide during combustion.^[4,5] So, while their end-use properties are vast and encompass a number of applications of societal importance, the overall life cycle of PUs must continue to be reevaluated in order to reduce their impact on our human health and the environment.

From a synthetic standpoint, a number of non-isocyanate routes to forming urethanes and polyurethanes have been undertaken, including various polycondensations and rearrangements, and the reader is directed toward several excellent reviews. [5-10] Of the many alternative routes described in the literature, the polyaddition of cyclic carbonates with diamines appears to be the most viable route for non-isocyanate polyurethanes (NIPUs). Cyclic carbonates are generally non-toxic and, once reacted with an amine, do not produce any byproducts. Many of the logistical and environmental benefits of utilizing cyclic carbonates over isocyanates to prepare polyurethanes was reviewed by Datta and

www.advancedsciencenews.com

Włoch.[11] Although cyclic carbonates have been and continue to be prepared from phosgene, phosgene derivatives, or epihalohydrins, carbon dioxide has been utilized in combination with epoxides, olefins or diols as a less hazardous approach.[12-14] For example, Torkelson and coworkers demonstrated that polyhydroxyurethane (PHU) thermoplastic elastomers could be prepared through the reaction of a mixture of cyclic carbonate-terminated PEG (poly(ethylene glycol)) and divinylbenzene dicyclocarbonate, prepared through CO2 insertion of the respective epoxide precursors, with 1,3-diaminopropane. [15] When compared with an analogous traditional PU made using isocyanate-polyol chemistry, they found that the PHU did not exhibit the same mechanical strength due to the presence of the free hydroxyl groups, formed during the ring-opening polymerization process. The hydroxyl groups prevented segregation of the soft and hard phases; however, phase mixing could be reduced when sterically hindered polyethers such as poly(propylene glycol) (PPG) or polyols with decreased ether content (PTMO - poly(tetramethylene oxide)) were used instead. In another example, plant oil-based 9-decenoate was epoxided and then converted into the cyclic carbonate by Long and coworkers.^[16] This difunctional material served as a key monomer in the synthesis of a series of poly(amide-hydroxyurethane)s. A more recent example of utilizing cyclic carbonates as monomers in the preparation of non-isocyanate polyurethanes involved the inclusion of dynamic disulfide bonds (cystamine), allowing for the recycling of the networks within 20 min at 100 °C.[17] A broad range of thermal and mechanical properties were realized by varying the nature of the difunctional cyclic carbonate monomer (PEG, PTMO, aromatic).

Yet another approach to making non-isocyanate polyurethanes involves the use of carbonyl diimidazole (CDI), a reagent historically used as an alternative to thionyl chloride or carbodiimides in the synthesis of amides and esters from carboxylic acids.[18-21] It has also been shown to have utility in the formation of ureas and urethanes.^[22,23] Compared to the cyclic carbonate approach previously described, the reaction of CDI avoids the use of catalysts such as DBU (1,8-diazabicyclo[5.4.0]undec-7-ene) which are required to promote polyaddition as well as the complication of phase mixing that often arises from the free hydroxyl group that is formed as a result of ring opening. CDI has been employed in polymerization reactions in the past, in particular the synthesis of polycarbonates.^[24,25] Dendritic and hyperbranched polyurethanes have also been prepared as reported by Rannard and coworkers, demonstrating that CDI can sequentially be reacted with an alcohol then an amine (or in the reverse) resulting in a urethane functional group.[26,27] More recently, Long et al. reported the first use of CDI in the synthesis of linear polyurethanes through the stepwise addition of 1,4-butanediol, forming an isolatable biscarbamate intermediate, followed by step-growth polymerization with a variety of diamines.^[28] The thermoplastic polyurethanes displayed high thermal stability ($T_{d5\%} > 275$ °C) and were melt processable.

Ionic liquid (IL)-containing polymers have applicability across a number of important applications, including carbon dioxide capture and energy storage. [29–32] IL-containing polymers can generally be divided into two architectures: poly(ionic liquid)s (PILs) where the IL group is pendant to the backbone and ionenes where the IL group is anchored directly into the backbone of the repeating unit. Early reports of polyurethane-containing ionenes

were reviewed by Nelson in 2014.[32] Since then, several research teams have focused on combining the hydrogen bonding capability of the urethane group and the ionic bonding displayed by the IL group to create unique materials for task-specific applications. For example, Morozova et al. disclosed a series of polyurethanes that combined various cations (ammonium, imidazolium, quinuclidinium) and anions ([BF₄], [PF₆], [NTf₂], and others) for carbon dioxide capture. [33] CO2 storage capacities of up to 24.8 mg g⁻¹ were observed for these materials. Spin-coated poly(acrylic acid)/polyurethane ammonium ionene films have also been disclosed, and were observed to exhibit self-healing properties due to the ability of the polyurethane to change conformations from a coiled to a stretched state, triggering long-distance polymer migration. [34] Shape memory and fixity properties have also been demonstrated for a series of ammonium IL-crosslinked polyurethanes.[35] Imidazolium-containing polyurethanes reported by Duan and workers not only high toughness and self-healing properties, but also antibacterial activity against S. aureus and E. coli. [36] Across all of these reports, the urethane groups were generated using isocyanate chemistry.

In this work, we report the synthesis of polyurethanes using a CDI non-isocyanate route which incorporate imidazolium ionic liquid (IL) units in the backbone, creating polyurethane ionenes. For the backbone, we utilized poly(propylene glycol) diols, which were subsequently reacted with CDI and 3-aminopropylimidazole (API), resulting in a series of imidazole-terminated polyurethane prepolymers. Stepgrowth Menshutkin polymerization, followed by anion exchange, resulted in a series of polyurethane ionenes bearing the bis(trifluoromethanesulfonyl)imide [NTf₂] counteranion. The polyurethane ionenes were characterized by NMR and IR spectroscopy, and analyzed for their thermal, morphological, and conductive properties. To the best of our knowledge, this represents the first report of IL-containing polyurethanes prepared using non-isocyanate chemistry.

2. Results and Discussion

2.1. Synthetic Approach

Polyurethane ionenes were prepared as follows. CDI was first reacted with poly(propylene glycol) (PPG) diols with various molecular weights (1100, 2000, 4100, 8000 g $\mathrm{mol^{-1}}$ as determined from end-group titration).[37] These reactions resulted in a series of biscarbonylimidazolide-terminated intermediates xK PPG-CDI where x refers to the molecular weight of the PPG used, i.e., 2 =2000 g mol⁻¹. These intermediates were then reacted with API (3-aminopropylimidazole), generating the urethane-containing prepolymers xK PPG-API bearing terminal imidazole groups. The prepolymers were then polymerized by coupling with 1,4dibromomethylbenzene in NMP at 150 °C at a 1:1 molar ratio of imidazole to bromide. The ionenes were isolated as the [NTf₂] derivatives by pouring the cooled reaction solution slowly into a solution of LiNTf, in DI water, allowing for removal of the solvent as well as anion exchange. The ionenes (xK PPG-ionene) were isolated as a series of viscous, light brown oils. The bromide ionene intermediates were not isolated as the overall goal of this study was to create materials that exhibited high thermal

15213935, 2023, 22, Downloaded from https://onlinelibrary.wikey.com/doi/10.1002/macp.202030290 by Murray State University, Wiley Commons in 25052024]. See the Terms and Conditions (https://onlinelibrary.wikey.com/rerms-and-conditions) on Wiley Online Library for rules of uses; OA articles are governed by the applicable Creative Commons in 25052024].

Scheme 1. Synthesis of poly(propylene glycol)-based polyurethane ionenes.

Table 1. Molecular weight data from ¹H NMR end-group analysis and thermal properties of the poly(propylene glycol) urethane-containing ionenes.

ionene	wt% PPG	¹ H NMR <i>M</i> _n (kg mol ⁻¹)	DSC T _g (°C)	TGA <i>T</i> _{d5%} (°C)
1K PPG-ionene	56	42.5	-38.1	251
2K PPG-ionene	70	41.2	-45.4	274
4K PPG-ionene	83	38.5	-58.9	280
8K PPG-ionene	90	51.8	-64.3	264

stability and ionic conductivity, both of which are enhanced with bulky, non-coordinating ions like [NTf₂] (**Scheme 1**).

2.2. Ionene Characterization and Thermal Properties

NMR and FTIR spectroscopies were used to confirm the identity and purity of the polymers as well as all of the corresponding intermediates. As the chemical shift of the end-group benzyl protons of the polyurethane ionenes (4.55 ppm in CDCl₃) in the ¹H NMR spectra were separate from the main chain signals, molecular weight values were determined by end-group analysis. The relative integration of the end-group benzyl signal was compared with that of the imidazolium H2 proton in the repeating unit of the ionene. A representative example (4K PPG-ionene) is shown in Figure 1. Molecular weight values are reported in Table 1 and ranged from 38.5–51.8 kg mol⁻¹. Additional NMR spectra can be found in the Supporting Information.

The polyurethane ionenes were also analyzed by FTIR spectroscopy and Figure 2 provides an overlay of the FTIR spectra for the 4K PPG polyurethane system as a representative example.

The **4K PPG-CDI** precursor displayed a sharp band corresponding to the carbonyl stretching at 1760 cm⁻¹ which shifted to lower wavenumber when the material was converted to **4K PPG-API** (1713 cm⁻¹) and final ionene (1706 cm⁻¹) versions, indicative of the formation of a urethane functional group. Also observed was the appearance of two bands corresponding to N-H stretching at 1534 and 1510 cm⁻¹ for **4K PPG-API** and 1562 and 1532 cm⁻¹ for **4K PPG-ionene**. The two N-H stretches are attributed to "free" and hydrogen-bound groups, respectively. These observations follow what other research teams have observed in their preparation of polyurethane ionenes. [33,37] Additionally, a series of new signals that are attributed to the [NTf₂] counteranion were observed in the final **4K PPG-ionene** product. These new bands include SO₂ stretching (1190 and 616 cm⁻¹), C-S stretching (788 cm⁻¹) and S-N-S stretching (740 and 640 cm⁻¹). [39,40]

Thermal properties of the ionenes were examined using differential scanning calorimetry (DSC) and thermogravimetric analysis (TGA). All four of the imidazolium polyurethane ionenes exhibited a single endothermic transition (–38 to –64 °C) corresponding to the glass transition temperature ($T_{\rm g}$) (**Figure 3**). Prior literature suggests that the closeness of the $T_{\rm g}$ values relative to that of pure PPG diol indicates microphase separation (for reference, a $T_{\rm g}$ value of –67.5 °C was found for the starting 4K PPG diol.). [37,38] Note that the ionene $T_{\rm g}$ values decrease and the transition sharpens as the PPG chain length increases, supporting this hypothesis. No other transitions (first or second heating) were observed for any of the samples. The presence of microphase separation will be revisited in the discussion of the X-ray scattering data.

Each of the polyurethane ionenes displayed a two-phase decomposition by TGA as shown in Figure 4. The first mass

15213935, 2023, 22, Dowlondedt from https://onlinelibarry.wiley.com/doi/10.1002/macp.202300290 by Murray State University, Wiley Online Libarry on [23/05/2024]. See the Terms and Conditions (https://onlinelibarry.wiley.com/terms

and-conditions) on Wiley Online Library for rules of use; OA articles are governed by the applicable Creative Commons

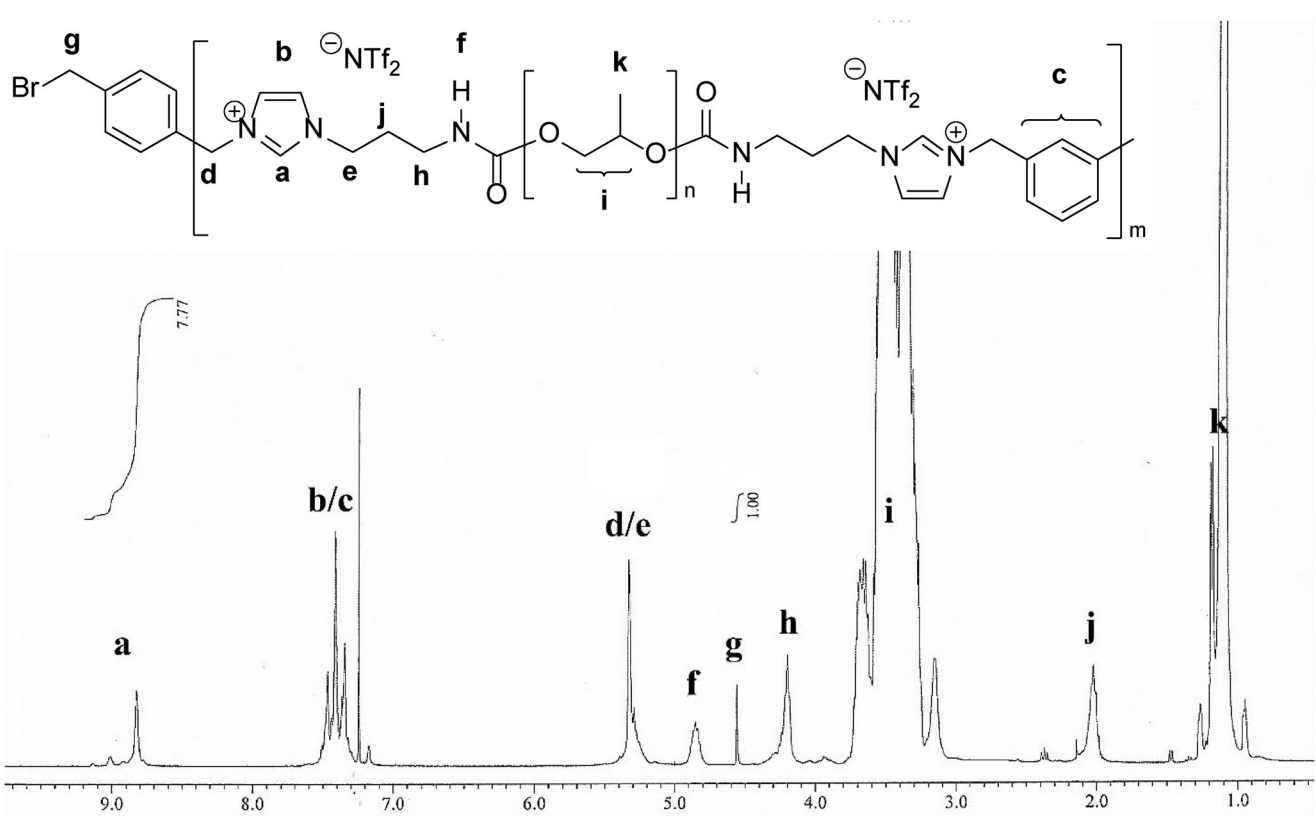
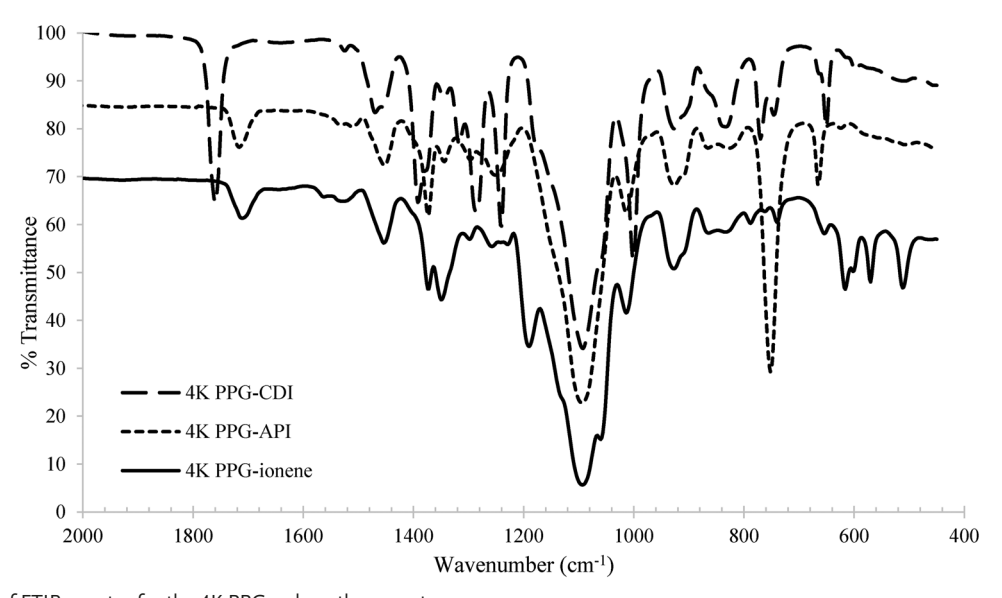


Figure 1. ¹H NMR spectrum of the **4K PPG-ionene** (in CDCl₃) with structural assignments. Integrations are provided for the end group benzylic protons **g** as well as the imidazolium protons **a**) of the repeating unit of the ionene.

loss (\approx 250 °C) is attributed to the decomposition of the poly(propylene glycol) backbone as this event matches accordingly with the wt.% PPG in each ionene (Table 1) and increases with increasing PPG chain length. For reference, the $T_{\rm d5\%}$ value observed for the 4K PPG starting diol was 220 °C. The second mass loss (\approx 340 °C) is assigned to the imidazolium/urethane

portion of the ionene which most likely occurs through a combination of retro- $S_{\rm N}2$ and elimination pathways; however, additional work beyond the scope of the present study would be necessary to confirm. Overall, the thermal stability of the polyurethane ionenes prepared was clearly limited by the PPG segment.



 $\textbf{Figure 2.} \ \ \text{Overlay of FTIR spectra for the 4K PPG-polyure than e system}.$

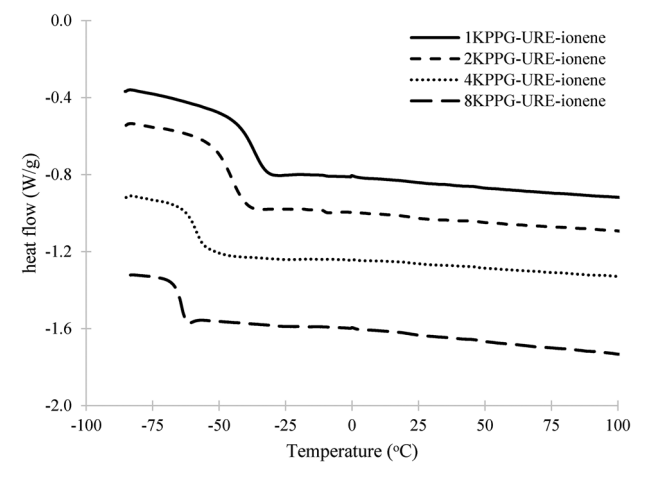


Figure 3. DSC overlay (second heating) of the imidazolium-containing ionenes.

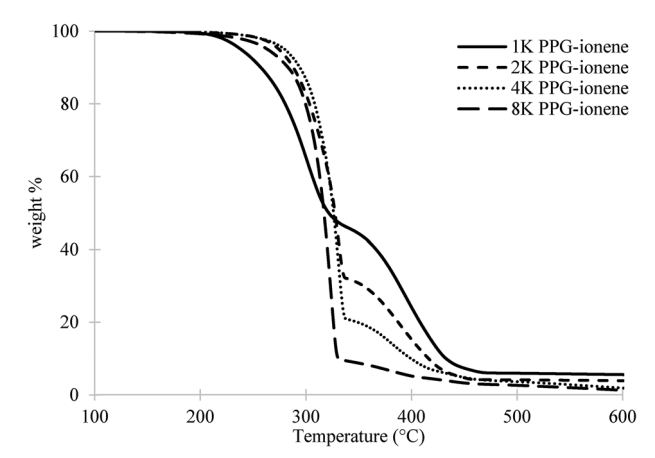


Figure 4. Thermogravimetric analysis data of the imidazolium-containing polyurethane ionenes.

2.3. Morphology

The polyurethane ionenes were also analyzed by x-ray scattering (WAXS/SAXS) in order to investigate their morphology. The x-ray scattering data shows three distinct peaks for each of the ionones (**Figure 5**). The high scattering vector (q_1) is assigned as the monomodal amorphous halo and is indicative of the amorphous nature of these materials. The scattering vector represents interactions between polymer backbones and cation/anion pairs apart from the neutral polymer. [38,40,41] The middle scattering vector (q_2) is associated with the distance between neighboring ionic groups (anion-anion and cation-cation) and is on the length scale (0.71 nm) reported for similar interactions in other PILs and ionenes. [$^{40-42}$] The low scattering vector (q_3) is the result of microphase separation between the hard and soft segments. Note that, starting with 1K PPG-ionene, there is broad gaussian-like curve indicate of a broad range of distances; however, as the length of the PPG chain gets longer, the peak becomes more prominent and shifts to lower q. This increase in intensity of q_3 is indicative of a higher degree of microphase separation due to an increase in electron density difference between the PPG segment and the urethane/ionic segment.[35,37,38] The correlated distances

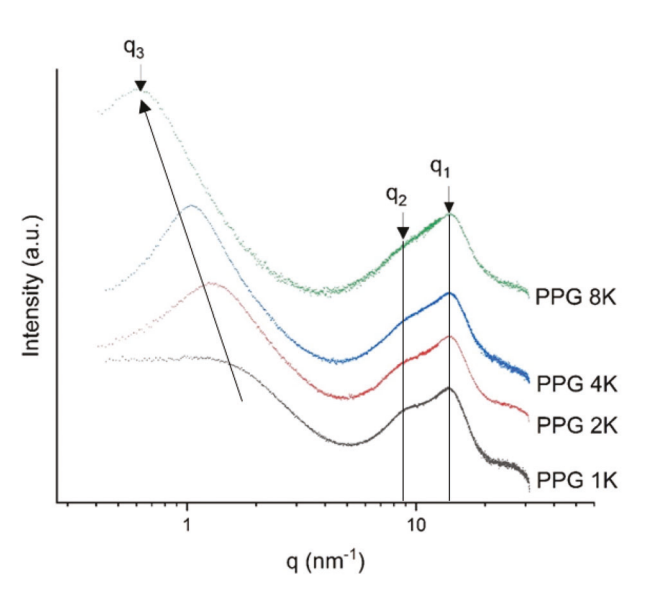


Figure 5. X-ray scattering (SAXS/WAXS) profiles for the poly(propylene glycol)-based polyurethane ionenes.

Table 2. X-ray scattering data for the polyurethane ionenes.

ionene	$q_1 \text{ (nm}^{-1}\text{)}$	$q_2 (nm^{-1})$	$q_3 \text{ (nm}^{-1}\text{)}$
1K PPG-ionene	13.9	8.9	1.53
2K PPG-ionene	13.9	8.9	1.33
4K PPG-ionene	13.9	8.9	1.05
8K PPG-ionene	13.9	8.9	0.62

calculated using Braggs Law for 1K PPG to 8K PPG goes from 4.0 to 10.1 nm, respectively. This assignment to microphase separation is corroborated by the differences in DSC $T_{\rm g}$ values. The **1K PPG-ionene** polyurethane has the highest $T_{\rm g}$ value of the series which would indicate significant mixing between the PPG and urethane/ionic phases. As microphase separation increases with increasing PPG chain length, the observed $T_{\rm g}$ decreases as it reflects the PPG segment (**Table 2**).

2.4. Ionic Conductivity

Conductivity of ion-containing polymers depends upon a number of factors including T_g , polymer morphology and structure, ion diffusion, and aggregation, and it is often difficult to separate which of these factors is the primary contributor. [41–47] Ionic conductivity values for each of the polyurethane ionenes were determined using a rheometer equipped with a dielectric accessory under an atmosphere of dry nitrogen. Each sample, at a thickness of 500 µm, was allowed to equilibrate at the desired temperature (90--30 in 10 °C steps) for 45 min prior to obtaining any data. As shown in Figure 6, ionic conductivity was found to be on the order of 10^{-4} to 10^{-5} S cm⁻¹ at 30 °C. At lower temperatures, closer to the polymers observed DSC $T_{\rm g}$ values, conductivity was found to be inversely related to $T_{\rm g}$ (8K > 4K > 2K > 1K). However, as the temperature increased, this trend eventually inverted with the 1K PPG-ionene being observed to have the highest ionic conductivity at 90°C (increasing to temperatures > 90 °C led to

Figure 6. Ionic conductivities of the poly(propylene glycol)-based, urethane-containing ionenes. Raw data points are provided along with VFT fitted solid curves.

sample flowing out from between the plates). In addition to the plotted data points in Figure 6, ionic conductivity curves were fitted with the Vogel–Fulcher–Tammann (VFT) equation as $\sigma_{\rm DC}$ values are dependent upon correlations between diffusion of the ionic species and polymer chain dynamics at temperatures above the $T_{\rm g}.^{[48,49]}$ The fitted data is represented by the solid curves shown in Figure 6 and the VFT fitting parameters are provided in the Supporting Information.

There are two primary, structural factors with these ionenes that dictate ionic conductivity: the PPG softer segment and the urethane/ionic harder segment. At lower temperatures, there must be restricted motion of the urethane/ionic harder segment, meaning that ionic conductivity is primarily driven by segmental relaxation of the softer PPG. The longer chain lengths (4K and 8K) provide more flexibility (reflected by the lower DSC T_{g} values) to allow for improved ion conduction. As the temperature increases, the urethane/ionic segments become more mobile and contribute more to the ionic conductivity; however, ion aggregation, caused by phase separation, dictates the ability of an ion to move from one aggregate to another. [46,47] In other words, longer PPG chain lengths force the ions into aggregates that are not well interconnected, leading to poor ion transport throughout the polymer matrix.[37] As 1K PPG-ionene utilizes the shortest PPG chain length and phase separation is not as defined, ions are not aggregated as well and/or the aggregates are interconnected (this distinction cannot be made at present), resulting in improved conductivity with temperature as well as the largest high-temperature ionic conductivity (σ_{∞} = 5.46 S/cm). It is also worth noting that the other ionenes (2 K, 4 K, and 8 K), all of which were observed to have a more definitive degree of phase separation by x-ray scattering, exhibit the same "crossover" temperature (≈10°C) whereby conductivity becomes more heavily dependent on the ability of ions to migrate from one aggregate to another as temperature increases. Long et al. have reported a similar dependence of ionic conductivity and temperature with regards to hard and soft segment $T_{\rm g}$ values and phase separation for a series of solid polyurethane ionomers bearing a PTMO soft segment.[38]

3. Conclusions

Polyurethanes are a vital class of polymers, and continue to be utilized in a number of commercial applications of societal importance. Despite their utility, the synthesis of polyurethanes remains highly hazardous due to the use of isocyanates. Several non-isocyanate pathways have been reported in the literature; however, each has their drawbacks such as the use of phosgene as a precursor or the need for a catalyst to promote polymerization. The use of carbonyldiimidazole (CDI) as a reagent represents yet another non-isocyanate alternative in which one can selectively chose the alcohol and amine partners in which to make the urethane. The process does not require a catalyst but isolation and scale-up evaluation of the imidazole byproduct formed as a result of each synthetic step needs further investigation.

In this report, we discuss the synthesis and characterization of a series of poly(propylene glycol) (PPG)-based polyurethane ionenes. CDI was first coupled with PPG diols with variable molecular weight, followed by reaction with 3-aminopropyl imidazole (API), generating imidazole-terminated urethanecontaining prepolymers. Menshutkin (S_N2) polymerization with 1,4-dibromomethylbenzene, followed by anion exchange with LiNTf₂, resulted in polyurethane ionenes. NMR and FTIR spectroscopy were used to confirm changes in chemical structure and ¹H NMR spectroscopy of the final ionenes were utilized to determine molecular weight (38.5–51.8 kg mol⁻¹) using end-group analysis. A single glass transition temperature (T_a) was observed for each ionene using DSC and values were found to decrease with increasing PPG molecular weight. This finding supports microphase separation of the PPG segment from the urethane/ionic segment. TGA results showed a two-phase degradation process for each ionene. The first event is assigned to the decomposition of the PPG segment as the mass percent lost matched the weight percent of the PPG contained in each ionene. The second decomposition event is assigned to the urethane/ionic segment, but additional studies would need to be completed to determine the exact mode of degradation.

The morphology of the polyurethane ionenes was investigated by small- and wide-angle X-ray scattering. Three distinct peaks were identified. The two high q signals (q_1 of 13.9 nm⁻¹ and q_2 of 8.9 nm⁻¹) are assigned to the amorphous halo and the ion-to-ion distances, respectively. These scattering distances did not change as a function of PPG molecular weight. The low q vector indicates microphase separation with correlated distances from 4.0 to 10.1 nm from the 1K to 8K PPG ionenes, respectively. As 1K PPG-ionene had the highest DSC T_g value and the smallest (and broadest) q_3 scattering vector, microphase separation was deemed to be the lowest in this polymer. Ionic conductivities were determined from 90 to −30 °C using the dielectric accessory of a rheometer under dry nitrogen conditions. At low temperatures, conductivity was found to increase with decreasing T_g as ion mobility is most likely linked to the relaxation of the PPG chains. As temperature increases and the urethane/ionic segment becomes more mobile, conductivity appears to be more dependent upon the ability of ions to move between segregated ionic clusters. Overall, this study represents the first report of polyurethane ionenes prepared using a non-isocyanate approach. Future work will focus on the ability to isolate the imidazole byproduct from the synthetic process,

thereby making the process more sustainable, and architectural changes that allow for greater mechanical stability of the ionenes, leading to potential application as membranes in energy devices.

4. Experimental Section

General: Several reagents used were purchased from TCI (carbonyl diimidazole (CDI)), Fisher Scientific (3-aminopropylimidazole (API), Nmethyl pyrrolidone (NMP)), or Pharmco (ethyl acetate, dichloromethane) and used as received. The poly(propylene glycol) (PPG) diols were provided by Bayer Scientific (Arcol 1000, Acclaims 2200, 4200, 8200). 1,4-Dibromomethylbenzene was prepared following a literature procedure. $^{[50]}$ Ultrapure water, having a resistivity of 18 M Ω -cm was produced using an ELGA Purelab Ultra filtration device. ¹H and ¹³C NMR spectra were acquired on a JEOL-ECS 400 MHz spectrometer and the chemical shift values reported are referenced to residual solvent signals in CDCl₂ (¹H, 7.26 ppm; ¹³C, 77.36 ppm).

Synthesis of 1K PPG-CDI: In a 100-mL round-bottomed flask equipped with a magnetic stir bar was dissolved the 1K PPG diol (Arcol® 1000; 10.00 g, 0.010 mol) in ethyl acetate (50 mL). CDI (4.05 g, 0.025 mol) was then added in portions over a 15-min period and the resulting solution was stirred at room temperature overnight. The reaction was then diluted with ethyl acetate (100 mL), transferred to a separatory funnel, and washed with DI water $(2 \times 50 \text{ mL})$, and brine (50 mL). The organic phase was isolated, dried over Na2SO4/MgSO4, filtered, and then the solvent was removed under reduced pressure to afford 10.32 g (86%) of a clear, colorless oil. ¹H NMR (CDCl₃): δ 8.09 (s, 2 H), 7.38 (s, 2 H), 7.01 (s, 2 H), 5.18 (bs, 2 H), 3.21-3.68 (m, $-CH_2-CH(CH_3)-O-$), 0.99-1.36 (m, $-CH_2-CH(CH_3)-O-$). ¹³C NMR (CDCl₃): δ 148.21, 137.04, 130.39, 117.08, 71.20-75.77 (-CH₂-CH(CH₃)-O-), 16.41-18.41 (-CH₂-CH(CH₃)-O-).

Synthesis of 1K PPG-API: In a 100-mL round-bottomed flask equipped with a magnetic stir bar was dissolved the carbonyl imidazole-terminated 1K PPG (10.00 g, 8.33 mmol) in dichloromethane (75 mL). API (3.12 g, 25.0 mmol) was added and the resulting solution was stirred at room temperature for 48 h. The solvent was then removed and the residue was dissolved in chloroform (100 mL) and washed with DI water (2 imes50 mL) and brine (50 mL). The organic phase was isolated and dried over Na2SO4/MgSO4, filtered, and the solvent was removed under reduced pressure to afford 9.92 g (92%) of a clear, colorless oil. $^1\mbox{H}$ NMR (CDCl₃): δ 7.46 (s, 2 H), 7.02 (s, 2 H), 6.91 (s, 2 H), 4.88 (bs, 2 H), 3.96 (t, 4 H, J = 7.1 Hz), 3.21-3.72 (m, -CH₂-CH(CH₃)-O-), 3.13 (m, 4 H), 1.95(t, 4 H, J = 6.8 Hz), 1.03-1.29 (m, -CH₂-CH(CH₃)-O-). ¹³C NMR (CDCl₃): δ 156.32, 137.04, 129.51, 118.75, 70.29-75.43 (-CH₂-CH(CH₃)-O-), 44.22, 37.87, 31.58, 16.92-18.23 (-CH₂-CH(*CH*₃)-O-).

Synthesis of the 1K PPG-ionene: In a PTFE screw-capped pressure vessel equipped with a magnetic stir bar was dissolved 1,4dibromomethylbenzene (0.99 g, 3.75 mmol) in NMP (30 mL). APIterminated 1K PPG (4.88 g, 3.75 mmol) was then added, and the reactor was sealed under argon and heated to 150 °C where it remained for 24 h. The reaction was then cooled to room temperature and slowly poured into a stirred solution of LiNTf₂ (6.49 g, 0.0225 mol) in DI water (100 mL). The resulting mixture was stirred for 24 h at room temperature. The water was then decanted and the residue was dissolved in dichloromethane (100 mL) and washed with DI water (2 \times 50 mL). The organic phase was then isolated and the solvent removed under reduced pressure to afford a viscous, light brown oil (4.65 g).

Synthesis of 2K PPG-CDI: In a 250-mL round-bottomed flask equipped with a magnetic stir bar was dissolved the 2K PPG diol (Acclaim® 2200, 5.00 g, 2.50 mmol) in ethyl acetate (50 mL). CDI (2.03 g, 12.50 mmol) was then added in portions over a 15 min period. The resulting solution was stirred at room temperature overnight. Additional ethyl acetate (50 mL) was then added, followed by transferring to a separatory funnel where it was washed sequentially with DI water (2×50 mL) and brine (50 mL). The organic phase was isolated, dried over Na₂SO₄/MgSO₄, filtered, and then the solvent was removed under reduced pressure to afford 5.35 g (97%) of a clear, colorless oil. ¹H NMR (CDCl₃): δ 8.14 (s, 2 H), 7.41 (s, 2 H), 7.04 (s, 2 H), 5.21 (bs, 2 H), 3.24-3.73 (m, -CH₂-CH(CH₃)-O-), 0.98-1.39 (m, $^{\circ}$ CH₂-CH(CH₃)-O-). 13 C NMR (CDCl₃): δ 148.16, 137.00, 130.23, 117.13, 71.11-75.86 (-CH₂-CH(CH₃)-O-), 16.40-18.47 (-CH₂-CH(CH₃)-O-)

Synthesis of 2K PPG-API: In a 100-mL round-bottomed flask equipped with a magnetic stir bar was dissolved the carbonyl imidazole-terminated 2K PPG (5.10 g, 2.32 mmol) in dichloromethane (50 mL). API (0.87 g, 6.95 mmol) was then added and the resulting solution was stirred at room temperature for 48 h. The solvent was then removed and the residue was dissolved in chloroform (50 mL) and washed with DI water (3 \times 50 mL), and brine (50 mL) in a separatory funnel. The organic phase was dried over Na₂SO₄/MgSO₄, filtered, and the solvent was removed under reduced pressure to afford 5.15 g (97%) of a clear, colorless oil. ¹H NMR (CDCl₃): δ 7.46 (s, 2 H), 6.98 (s, 2 H), 6.88 (s, 2 H), 4.84 (bs, 2 H), 3.93 (t, 4 H, I = 7.0 Hz), 3.20-3.70 (m, -CH₂-CH(CH₃)-O-), 3.11 (m, 4 H), 1.92(t, 4 H, J = 6.6 Hz), 0.91-1.26 (m, -CH₂-CH(CH₃)-O-). ¹³C NMR (CDCl₃): δ 156.26, 136.94, 129.30, 118.69, 70.22-75.34 (-CH₂-CH(CH₂)-O-), 44.16, 37.76, 31.49, 16.86-18.37 (-CH₂-CH(CH₃)-O-).

Synthesis of the 2K PPG-ionene: In a PTFE screw-capped pressure vessel equipped with a magnetic stir bar was dissolved 1,4dibromomethylbenzene (0.34 g, 1.30 mmol) in NMP (20 mL). APIterminated 2K PPG (3.00 g, 1.30 mmol) was then added, and the reactor was sealed under argon and heated to 150 °C where it remained for 24 h. The reaction was then cooled to room temperature and slowly poured into a stirred solution of LiNTf₂ (2.25 g, 7.83 mmol) in DI water (75 mL). The resulting mixture was stirred for 24 h at room temperature. The water was then decanted and the residue was dissolved in dichloromethane (100 mL) and washed with DI water (2 × 50 mL). The organic phase was then isolated and the solvent removed under reduced pressure to afford a viscous, light brown oil (3.02 g).

Synthesis of 4K PPG-CDI: In a 250-mL round-bottomed flask equipped with a magnetic stir bar was dissolved the 4K PPG diol (Acclaim® 4200,10.00 g, 2.50 mmol) in ethyl acetate (100 mL). CDI (2.03 g, 12.50 mmol) was then added in portions over a 15 min period. The resulting solution was stirred at room temperature overnight. It was then transferred to a separatory funnel where it was washed sequentially with DI water (50 mL), 5% NaCl solution (50 mL), and brine (50 mL). The organic phase was isolated, dried over Na2SO4/MgSO4, filtered, and then the solvent was removed under reduced pressure to afford 10.37 g (99%) of a clear, colorless oil. 1 H NMR (CDCl₃): δ 8.10 (s, 2 H), 7.39 (s, 2 H), 7.02 (s, 2 H), 5.21 (bs, 2 H), 3.21-3.72 (m, -CH₂-CH(CH₃)-O-), 0.98-1.36 (m, -CH₂-CH(CH_2)-O-). ¹³C NMR (CDCl₃): δ 148.20, 137.04, 130.38, 117.08, 72.7-75.9 (-CH₂-CH(CH₃)-O-), 16.4-18.6 (-CH₂-CH(CH₃)-O-).

Synthesis of 4K PPG-API: In a 250-mL round-bottomed flask equipped with a magnetic stir bar was dissolved the carbonyl imidazole-terminated 4K PPG (10.00 g, 2.38 mmol) in dichloromethane (75 mL). API (1.49 g, 11.9 mmol) was then added and the resulting solution was stirred at room temperature for 48 h. The solvent was then removed and the residue was dissolved in chloroform (100 mL) and washed with DI water (2×50 mL), and brine (50 mL) in a separatory funnel. The organic phase was then dried over Na₂SO₄/MgSO₄, filtered, and the solvent was removed under reduced pressure to afford 10.07 g (98%) of a clear, colorless oil. ¹H NMR $(CDCl_3)$: δ 8.07 (bs, 2 H), 7.13 (s, 2 H), 7.04 (s, 2 H), 5.88 (bs, 2 H), 4.08 (t, 4 H, J = 7.0 Hz), 3.25-3.75 (m, -CH₂-CH(CH₃)-O-), 3.17 (m, 4 H), 2.00(t, 4 H, J = 6.7 Hz), 1.06-1.29 (m, -CH₂-CH(CH₃)-O-). ¹³C NMR (CDCl₃): δ 156.30, 136.97, 129.30, 11877, 71.80-75.74 (-CH₂-CH(CH₃)-O-), 44.3, 37.84, 31.57, 16.89-18.43 (-CH₂-CH(CH₃)-O-).

Synthesis of the 4K PPG-ionene: In a PTFE screw-capped pressure vessel equipped with a magnetic stir bar was dissolved 1,4dibromomethylbenzene (0.18 g, 0.70 mmol) in NMP (20 mL). APIterminated 4K PPG (3.00 g, 0.70 mmol) was then added, and the reactor was sealed under argon and heated to 150 °C where it remained for 24 h. The reaction was then cooled to room temperature and slowly poured into a stirred solution of LiNTf₂ (1.20 g, 4.19 mmol) in DI water (100 mL). The resulting mixture was stirred for 24 h at room temperature. The water was then decanted and the residue was dissolved in dichloromethane (100 mL) and washed with DI water (2 × 50 mL). The organic phase was then isolated and the solvent removed under reduced pressure to afford a viscous, light brown oil (2.85 g).

under an atmosphere of dry nitrogen. Temperature was controlled using the environmental chamber in combination with liquid nitrogen. Dielectric permittivity and conductivity were measured isothermally over a frequency range of 20.0–10 6 Hz in 10 $^\circ$ C steps with an ac amplitude of ± 0.01 V from 90 to -30 °C. Samples were soaked at each temperature for 45 min prior to obtaining measurements. The DC conductivity ($\sigma_{\rm DC}$) was determined from the plateau value observed in the spectral dependence of the conductivity function ($\sigma' = \omega \varepsilon'' \varepsilon_{\rm o}$, where ω is the frequency, ε'' is the dielectric loss, and $\varepsilon_{\rm o}$ is the vacuum permittivity).

Synthesis of 8K PPG-CDI: In a 100-mL round-bottomed flask equipped with a magnetic stir bar was dissolved the 8K PPG diol (Acclaim® 8200; 5.00 g, 0.625 mmol) in ethyl acetate (50 mL). CDI (0.51 g, 3.13 mmol) was then added in portions over a 15 min period. The resulting solution was stirred at room temperature overnight. It was then transferred to a separatory funnel where it was diluted with additional ethyl acetate (100 mL) and washed sequentially with DI water (50 mL), 5% NaCl solution (50 mL), and brine (50 mL). The organic phase was isolated, dried over Na₂SO₄/MgSO₄, filtered, and then the solvent was removed under reduced pressure to afford 4.95 g (95%) of a clear, colorless oil. ¹H NMR (CDCl₃): δ 8.15 (s, 2 H), 7.41 (s, 2 H), 7.05 (s, 2 H), 5.21 (bs, 2 H), 3.21-3.73 (m, -CH₂-CH(CH₃)-O-), 0.91-1.41 (m, -CH₂-CH(CH₃)-O-). ¹³C NMR (CDCl₃): δ 148.19, 137.03, 130.30, 117.12, 72.76-75.45 (-CH₂-CH(CH₃)-O-), 16.46-18.46 (-CH₂-CH(CH₃)-O-)

Synthesis of 8K PPG-API: In a 100-mL round-bottomed flask equipped with a magnetic stir bar was dissolved the carbonyl imidazole-terminated 8K PPG (2.90 g, 0.35 mmol) in dichloromethane (25 mL). API (0.27 g, 2.12 mmol) was then added and the resulting solution was stirred at room temperature for 48 hr. The solvent was then removed and the residue was dissolved in chloroform (50 mL) and washed with DI water (2 × 30 mL), and brine (30 mL). The organic phase was then dried over Na₂SO₄/MgSO₄, filtered, and the solvent was removed under reduced pressure to afford 2.76 g (94%) of a clear, colorless oil. ¹H NMR (CDCl₃): δ 7.60 (bs, 2 H), 7.04 (s, 2 H), 6.93 (s, 2 H), 4.88 (bs, 2 H), 4.00 (t, 4 H, J=6.8 Hz), 3.22-3.71 (m, -CH₂-CH(CH₃)-O-), 3.17 (m, 4 H), 1.96 (t, 4 H, J=7.0) Hz), 0.93-1.28 (m, -CH₂-CH(CH₃)-O-). ¹³C NMR (CDCl₃): δ 156.22, 136.89, 129.29, 118.63, 70.40-75.64 (-CH₂-CH(CH₃)-O-), 44.12, 37.72, 31.49, 17.04-18.32 (-CH₂-CH(CH₃)-O-).

Synthesis of the 8K PPG-ionene: In a PTFE screw-capped pressure vessel equipped with a magnetic stir bar was dissolved 1,4-dibromomethylbenzene (95.1 mg, 0.36 mmol) in NMP (20 mL). API-terminated 8K PPG (3.00 g, 0.36 mmol) was then added, and the reactor was sealed under argon and heated to 150 °C where it remained for 24 h. The reaction was then cooled to room temperature and slowly poured into a stirred solution of LiNTf₂ (0.62 g, 2.16 mmol) in DI water (75 mL). The resulting mixture was stirred for 24 h at room temperature. The water was then decanted and the residue was dissolved in dichloromethane (100 mL) and washed with DI water (2 × 50 mL). The organic phase was then isolated and the solvent removed under reduced pressure to afford a viscous brown oil (2.78 g).

Thermal Analysis: Differential scanning calorimetry (DSC) was utilized to determine any thermal transitions of the polymers at a heating rate of 2 $^{\circ}$ C min $^{-1}$ on 3–8 mg samples. Glass transition temperatures (T_g) were determined by the inflection point of the curve observed from the second heating cycle. All DSC T_g experiments were performed in duplicate with an error of $\pm 2.0\,^{\circ}$ C. A TA instruments Q550 TGA (thermogravimetric analyzer) was used to evaluate $T_{d5\%}$ values (the temperature at which 5% of the material had decomposed) by heating the material under a constant dry nitrogen flow at a heating rate of 10 $^{\circ}$ C min $^{-1}$.

X-Ray Scattering Data: Morphological studies were conducted using a Xeuss 2.0 Dual Source Environmental X-ray Scattering system at the University of Pennsylvania. Data acquisition was performed under a vacuum. A copper X-ray source was used for incident radiation, and a 1 M Pilatus solid-state detector was used for wide-angle scattering (WAXS); $\lambda = 1.54189$ Å. Acquisition of data was performed for samples using full flux collimation with a 1.2 mm x 1.2 mm slit for a 600 s scan time. Using Datasqueeze 3.0, isotropic 2-D scattering patterns were converted by azimuthal integration to yield a 1-D profile of intensity (a.u.) versus scattering vector q (nm $^{-1}$). Bragg's equation was used to calculate values for d-spacing.

Conductivity: Anhydrous ionic conductivities were measured using a TA Instruments DHR-2 discovery hybrid rheometer equipped with a dielectric accessory and a Keysight Technologies E4980AL/120 LCR meter was utilized. Each ionene sample was first dried in a vacuum oven for 48 h (60 °C, < 0.1 mm Hg) for 48 hours. Then, the sample was placed between two 25 mm stainless steel parallel plate electrodes and the gap set to 500 μ m. Any excess material (squeeze out) was carefully removed with a PFTE razor blade. The environmental chamber was closed and kept

Supporting Information

Supporting Information is available from the Wiley Online Library or from the author.

Acknowledgements

The authors would like to thank the Committee on Institutional Studies and Research (CISR) at Murray State University for partial financial support of this work. Partial financial support was also provided by NSF-CMMI (2037097) and NSF-DMR (2104376). A special thank you for the acquisition of X-ray scattering data by Abneris Morales and Creston Singer, Ph.D. students of the Center for Computational and Integrative Biology at Rutgers University—Camden. The DEXS System is supported by NSF-MRSEC 17—20530, NSF-MRI 17—25969, ARO DURIP W911NF-17-1-02822, and the University of Pennsylvania.

Conflict of Interest

The authors declare no conflict of interest.

Data Availability Statement

The data that support the findings of this study are available in the supplementary material of this article.

Keywords

ionene, non-isocyanate, polyurethane, structure-activity relationship

Received: August 9, 2023 Revised: September 6, 2023 Published online: September 21, 2023

- [1] O. Bayer, Angew. Chem. 1947, 49, 257.
- [2] D. Bello, C. A. Herrick, T. J. Smith, S. R. Woskie, R. P. Streicher, M. R. Cullen, Y. Liu, C. A. Redlich, Environ. Health Perspect. 2007, 115, 328.
- [3] J. E. Doe, H. D. Hoffmann, Toxicol Ind Health 1995, 11, 13.
- [4] A. Cornille, C. Guillet, S. Benyahya, C. Negrell, S. Caillol, Eur. Polym. J. 2016, 86, 873.
- [5] A. Cornille, R. Auvergne, O. Figovsky, B. Boutevin, S. Caillol, Eur. Polym. J. 2017, 87, 535.
- [6] J. Guan, Y. Song, Y. Lin, X. Yin, X. Yin, M. Zuo, Y. Zhao, X. Tao, Q. Zheng, Ind. Eng. Chem. Res. 2011, 50, 6517.
- [7] M. S. Kathalewar, P. B. Joshi, A. S. Sabnis, V. C. Malshe, RSC Adv. 2013, 3, 4110.
- [8] G. Rokicki, P. G. Parzuchowski, M. Mazurek, Polym. Adv. Technol. 2015, 26, 707.

www.advancedsciencenews.com

- [9] H. Sardon, A. Pascual, D. Mecerreyes, D. Taton, H. Cramail, J. L. Hedrick, Macromolecules 2015, 48, 3153.
- [10] H. Khatoon, S. Iqbal, M. Irfan, A. Darda, N. K. Rawat, Prog. Org. Coat. 2021, 154, 106124.
- [11] J. Datta, M. Włoch, Polym. Bull. 2016, 73, 1459.
- [12] A. Dibenedetto, A. Angelini, Adv. Inorg. Chem. 2014, 66, 25.
- [13] H. Blattmann, M. Fleischer, M. Bähr, R. Mülhaupt, Macromol. Rapid Commun. 2014, 35, 1238.
- [14] M. Ghasemlou, F. Daver, E. P. Ivanova, B. Adhikari, Eur. Polym. J. 2019, 118, 668.
- [15] E. K. Leitsch, G. Beniah, K. Liu, T. Lan, W. H. Heath, K. A. Scheidt, J. M. Torkelson, ACS Macro Lett 2016, 5, 424.
- [16] K. Zhang, A. M. Nelson, S. J. Talley, M. Chen, E. Margaretta, A. G. Hudson, R. B. Moore, T. E. Long, Green Chem. 2016, 18, 4667.
- [17] C. Pronoitis, M. Hakkarainen, K. Odelis, ACS Sustainable Chem. Eng. 2022, 10, 2522.
- [18] A. Armstrong, W. Li, Encyclopedia of Reagents for Organic Synthesis, (Ed.: L. A. Paquette), John Wiley and Sons, Chichester, 1995, Vol. 2, p. 1006.
- [19] J. D. White, S. N. Lodwig, G. L. Trammell, M. P. Fleming, Tetrahedron Lett. 1974, 15, 3263.
- [20] R. Vaidyanathan, V. G. Kalthod, D. P. Ngo, J. M. Manley, S. P. Lapekas, J. Org. Chem. 2004, 69, 2565.
- [21] S. T. Heller, R. Sarpong, Org. Lett. 2010, 12, 4572.
- [22] K. J. Padiya, S. Gavade, B. Kardile, M. Tiwari, S. Bajare, M. Mane, V. Gaware, S. Varghese, D. Harel, S. Kurhade, Org. Lett. 2012, 14, 2814.
- [23] J. Bansagi, C. Wilson-Konderka, V. Debrauwer, P. Narayanan, R. A. Batey, J. Org. Chem. 2022, 87, 11329.
- [24] F. M. Houlihan, F. Bouchard, J. M. J. Frechet, C. G. Willson, Macromolecules 1986, 19, 13.
- [25] E. W. P. Tan, J. L. Hedrick, P. L. Arrechea, T. Erdmann, V. Kiyek, S. Lottier, Y. Y. Yang, N. H. Park, Macromolecules 2021, 54, 1767.
- [26] W. J. Feast, S. P. Rannard, A. Stoddart, Macromolecules 2003, 36, 9704.
- [27] S. P. Rannard, N. J. Davis, I. Herbert, Macromolecules 2004, 37, 9418.
- [28] J. D. Wolfgang, B. T. White, T. E. Long, Macromol. Rapid Commun. 2021, 42, 2100163.
- [29] S. Zhang, Q. Zhuang, M. Zhang, H. Wang, Z. Gao, J. Sun, J. Yuan, Chem. Soc. Rev. 2020, 49, 1726.

- [30] S. Zulfigar, M. I. Sarwar, D. Mecerreyes, Polym. Chem. 2015, 6, 6435.
- [31] J. E. Bara, K. E. O'Harra, Macromol. Chem. Phys. 2019, 220, 1900078.
- [32] A. M. Nelson, T. E. Long, Macromol. Chem. Phys. 2014, 215, 2161.
- [33] S. M. Morozova, A. S. Shaplov, E. I. Lozinskaya, D. Mecerreyes, H. Sardon, S. Zulfiqar, F. Suárez-García, Y. S. Vygodskii, *Macromolecules* 2017, 50, 2814.
- [34] Y. Wang, M. Zheng, X. Wang, S. Li, J. Sun, ACS Appl. Mater. Interfaces 2018. 10. 30716.
- [35] P. K. Behera, P. Mondal, N. K. Singha, Polym. Chem. 2018, 9, 4205.
- [36] N. Duan, Z. Sun, Y. Ren, Z. Liu, L. Liu, F. Yan, *Polym. Chem.* **2020**, *11*, 867
- [37] M. Tamani, S. R. Williams, J. K. Park, R. B. Moore, T. E. Long, J. Polym. Sci., Part A: Polym. Chem. 2010, 48, 4159.
- [38] R. Gao, M. Zhang, S. Wang, R. B. Moore, R. H. Colby, T. E. Long, Macromol. Chem. Phys. 2013, 214, 1027.
- [39] V. H. Paschoal, L. F. O. Faria, M. C. C. Ribiero, Chem. Rev. 2017, 117, 7053.
- [40] R. J. Miller, V. M. Smith, S. A. Love, S. M. Byron, D. Salas-de la Cruz, K. M. Miller, ACS Appl. Polm. Mater. 2021, 3, 1097.
- [41] U. H. Choi, Y. Ye, D. Salas-de la Cruz, W. Liu, K. I. Winey, Y. A. Elabd, J. Runt, R. H. Colby, Macromolecules 2014, 47, 777.
- [42] D. Salas-de la Cruz, M. D. Green, Y. Ye, Y. A. Elabd, T. E. Long, K. I. Winey, J. Polym. Sci., Part B: Polym. Phys. 2012, 50, 338.
- [43] J. R. Keith, N. J. Rebello, B. J. Cowen, V. Ganesan, ACS Macro Lett. 2019, 8, 387.
- [44] L. J. Abbott, J. W. Lawson, Macromolecules 2019, 52, 7456.
- [45] E. W. Stacy, C. P. Gainaru, M. Gobet, Z. Wojnarowska, V. Bocharova, S. G. Greenbaum, A. P. Sokolov, *Macromolecules* 2018, 51, 8637.
- [46] B. K. Wheatle, N. A. Lynd, V. Ganesan, ACS Macro Lett. 2018, 7, 1149.
- [47] N. S. Schauser, D. J. Grzetic, T. Tabasum, G. A. Kliegle, N. L. Le, E. M. Susca, S. Antoine, T. J. Keller, K. T. Delaney, S. Han, R. Seshardi, G. H. Fredrickson, R. A. Segalman, J. Am. Chem. Soc. 2020, 142, 7055
- [48] C. Jangu, J. H. Wang, D. Wang, S. Sharick, J. R. Haflin, K. I. Winey, R. H. Colby, T. E. Long, *Macromol. Chem. Phys.* 2014, 215, 1319.
- [49] N. C. Bontrager, S. Radomski, S. P. Daymon, R. D. Johnson, K. M. Miller, *Polymer* 2021, 222, 123641.
- [50] C. Liu, C.-C. Wang, D.-L. Kuo, C.-Y. Yu, Polymer 2019, 181, 121770.